ELSEVIER

Journal of Volcanology and Geothermal Research 114 (2002) 291–312

Journal of volcanology and geothermal research

www.elsevier.com/locate/jvolgeores

Tracing and quantifying magmatic carbon discharge in cold groundwaters: lessons learned from Mammoth Mountain, USA

William C. Evans [a,*], Michael L. Sorey [a], Andrea C. Cook [b], B. Mack Kennedy [c], David L. Shuster [c], Elizabeth M. Colvard [a], Lloyd D. White [a], Mark A. Huebner [a]

[a] *US Geological Survey, 345 Middlefield Road, Menlo Park, CA 94025, USA*
[b] *Lawrence Livermore National Laboratory, Center for Accelerator Mass Spectrometry, Livermore, CA 94551, USA*
[c] *Lawrence Berkeley National Laboratory, Center for Isotope Geochemistry, Berkeley, CA 94701, USA*

Received 10 January 2001; received in revised form 13 June 2001; accepted 13 June 2001

Abstract

A major campaign to quantify the magmatic carbon discharge in cold groundwaters around Mammoth Mountain volcano in eastern California was carried out from 1996 to 1999. The total water flow from all sampled cold springs was $\geq 1.8\times10^7$ m^3/yr draining an area that receives an estimated 2.5×10^7 m^3/yr of recharge, suggesting that sample coverage of the groundwater system was essentially complete. Some of the waters contain magmatic helium with ^{3}He/^{4}He ratios as high as 4.5 times the atmospheric ratio, and a magmatic component in the dissolved inorganic carbon (DIC) can be identified in virtually every feature sampled. Many waters have a ^{14}C of 0–5 pmC, a δ^{13}C near -5‰, and contain high concentrations (20–50 mmol/l) of $CO_{2(aq)}$; but are otherwise dilute (specific conductance = 100–300 μS/cm) with low pH values between 5 and 6. Such waters have previously escaped notice at Mammoth Mountain, and possibly at many other volcanoes, because CO_2 is rapidly lost to the air as the water flows away from the springs, leaving neutral pH waters containing only 1–3 mmol/l HCO_3^-. The total discharge of magmatic carbon in the cold groundwater system at Mammoth Mountain is ~20 000 t/yr (as CO_2), ranging seasonally from about 30 to 90 t/day. Several types of evidence show that this high discharge of magmatic DIC arose in part because of shallow dike intrusion in 1989, but also demonstrate that a long-term discharge possibly half this magnitude (~10 000 t/yr) predated that intrusion. To sustain a 10 000 t/yr DIC discharge would require a magma intrusion rate of 0.057 km^3 per century, assuming complete degassing of magma with 0.65 wt% CO_2 and a density of 2.7 t/m^3. The geochemical data also identify a small (< 1 t/day) discharge of magmatic DIC that can be traced to the Inyo Domes area north of Mammoth Mountain and outside the associated Long Valley caldera. This research, along with recent studies at Lassen Peak and other western USA volcanoes, suggests that the amount of magmatic carbon in cold groundwaters is important to constraining rates of intrusion and edifice weathering at individual volcanoes and may even represent a significant fraction of the global carbon discharge from volcanoes.

* Corresponding author. Fax: +1-650-329-4463. *E-mail address:* wcevans@usgs.gov (W.C. Evans).

0377-0273/02/$ – see front matter
PII: S0377-0273(01)00268-2

Keywords: volcanoes; groundwater; magmatic gas; carbon dioxide

1. Introduction

Volcanoes have long been known to sustain sizeable emissions of gas during periods of dormancy, most visibly evidenced by fumaroles and bubbling hot springs. Recent studies of gas released diffusely through flank emissions or in cold groundwaters suggest that these not so visible components of magmatic gas are seriously underestimated, or their effects on health hazards and water quality under appreciated, on a global basis (e.g. Baubron et al., 1990; Allard et al., 1991; Farrar et al., 1995; Rose and Davisson, 1996; Giammanco et al., 1998; Chiodini et al., 1999; Baxter et al., 1999; Werner et al., 2000; Williams-Jones et al., 2000). Mammoth Mountain, in eastern California, provides an important case study. This Quaternary volcano has been emitting hundreds of tons of CO_2 per day through normal-temperature soils for over a decade following a small dike intrusion in 1989. The death of $\sim$50 ha of coniferous forest on the slopes of the edifice provided a highly visible sign of the diffuse emissions (Farrar et al., 1995). Many subsequent studies have focused on identifying the source of that gas and on quantifying the total diffuse emission of CO_2 (Rahn et al., 1996; Farrar et al., 1998; Sorey et al., 1998; Gerlach et al., 2001).

A reconnaissance sampling of groundwaters showed that many of the cold springs and wells lower on the flanks of Mammoth Mountain were rich in dissolved CO_2; some features were effervescent. In many waters, the dissolved inorganic carbon (DIC), comprising the CO_2 and resultant HCO_3^-, had a $\delta^{13}C$ near $-5‰$, similar to the $\delta^{13}C$ of the magmatic CO_2 in steam vents high on the mountain and in soil CO_2 within the tree-kill areas. A preliminary estimate of the total discharge of magmatic carbon in the groundwater system was given as 30–50 t/day (as CO_2) by Sorey et al. (1998). A comprehensive sampling and stream gaging program, carried out over the past few years, allows us to now refine this estimate. The CO_2-rich waters fall into the 'immature-' or 'peripheral-water' category of Giggenbach (1988), but examples as dilute as these are infrequently reported in the literature. To support our contention that magmatic carbon discharge in such dilute waters could be greatly overlooked at even well-studied volcanoes, we review the evidence that the CO_2 anomaly in some of these features at Mammoth Mountain long predates the 1989 intrusion, and we discuss our recent discovery of similar discharges of cold, CO_2-rich water at Lassen volcano, 400 km to the northwest.

2. Study area

2.1. Geologic setting and volcanic history

The study area and sample sites are shown in Fig. 1. Precise locations, elevations, and additional geochemical data are available at (http://wwwrcamnl.wr.usgs.gov/volcwater). This site also shows high-resolution topographic and geologic maps.

The regional geology and volcanic history have been presented by Bailey (1989). Mammoth Mountain rises from the rim of the 760 kyr Long Valley caldera, but also lies at the southern end of the Inyo volcanic chain. Regional volcanism over the past 40 000 yr has been focused along this chain, with $\sim$700 yr phreatic eruptions on the north side of Mammoth Mountain preceding the most recent Inyo chain eruptions (Sorey et al.,

Fig. 1. Long Valley caldera and groundwater sampling locations. Heavy solid line at Mammoth Mountain shows 2900-m elevation contour. Diamonds denote areas of tree kill. The major exposures of Paleozoic meta-sedimentary (Pzms), Mesozoic meta-volcanic (Mzmv), and Cretaceous granitic (Kg) rocks are shown (from Bailey, 1989). Remaining area consists mainly of Quaternary and some Tertiary volcanics, with two of the larger andesite flows (Qa) and the rhyolitic Inyo Volcanic chain (Qr) shown (from Bailey, 1989). Town of Mammoth Lakes, main ski lodge, MMF, resurgent dome, and 40 MWe geothermal power plant at Casa Diablo are also shown.

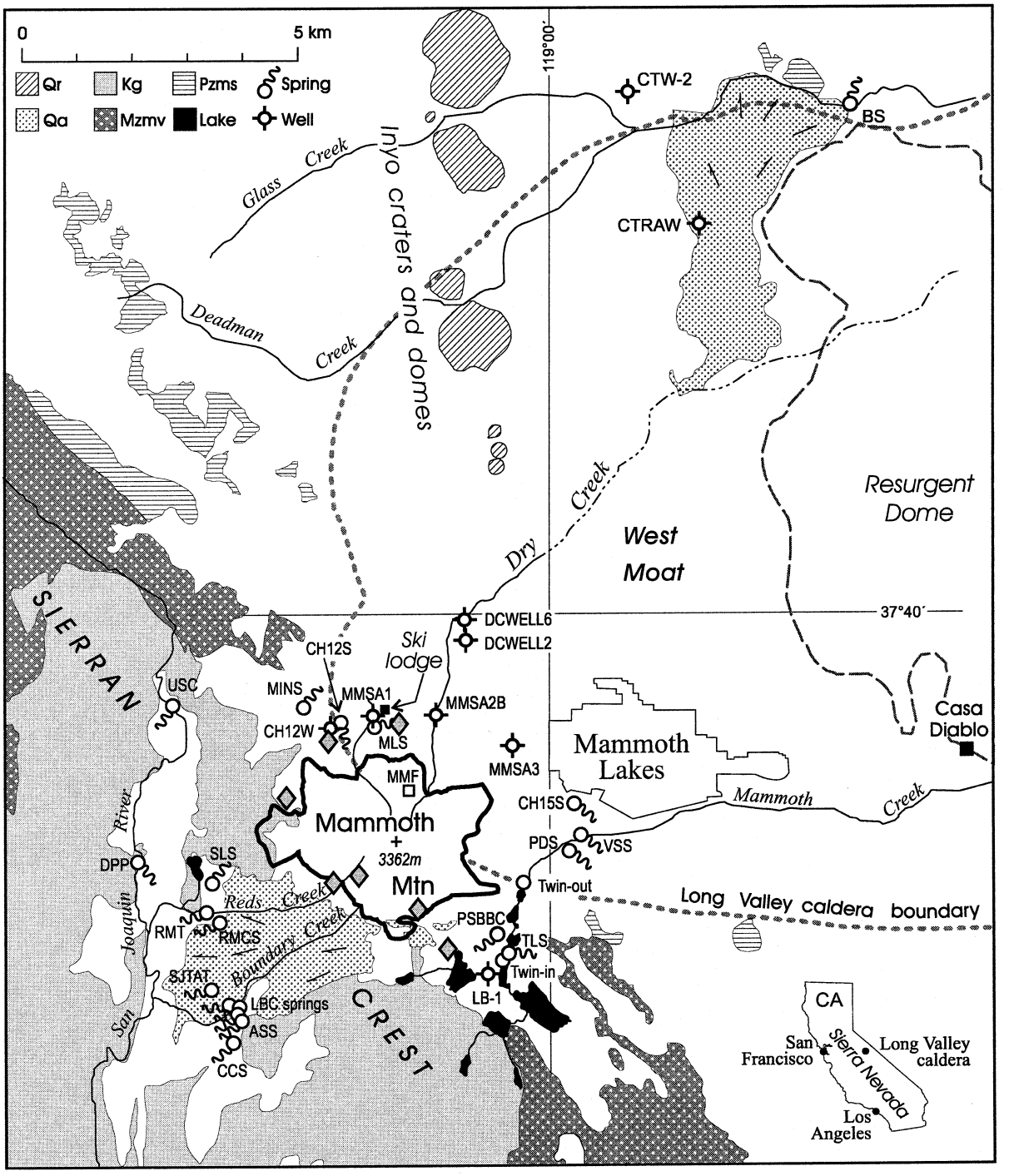
0
5 km
Qr
Kg
Pzms
Spring
Qa
Mzmv
Lake
Well
119°00´
CTW-2
BS
CTRAW
Glass Creek
Inyo craters and domes
Deadman Creek
Dry Creek
Resurgent Dome
West Moat
37°40´
SIERRAN
DCWELL6
DCWELL2
CH12S
Ski lodge
USC
MINS
MMSA1
MMSA2B
CH12W
MLS
MMSA3
MMF
Mammoth Lakes
Casa Diablo
CH15S
Mammoth Creek
Mammoth + 3362m Mtn
PDS
VSS
DPP
SLS
River
Joaquin
Reds Creek
Twin-out
Long Valley caldera boundary
RMT
RMCS
Boundary Creek
PSBBC
TLS
SJTAT
Twin-in
LB-1
LBC springs
San
ASS
CCS
CREST
CA
San Francisco
Sierra Nevada
Long Valley caldera
Los Angeles

1998). Silicic rocks form the edifice of Mammoth Mountain, but basalts crop out in places near the base, and extensive basalt flows have been encountered in boreholes within the West Moat of the caldera. The mountain is bordered on the west and south by granitic rocks of the Sierran block, but Tertiary volcanics, Mesozoic meta-volcanics, and Paleozoic meta-sediments (including carbonates; see White et al., 1990) are exposed widely in the region. The deep reservoir and upflow zone of the large hydrothermal system in the caldera is apparently hosted in meta-sedimentary basement beneath the West Moat (Sorey et al., 1991).

2.2. Hydrology

Mammoth Mountain forms part of the Sierran crest and receives heavy snowfall. The ground surface is highly permeable to infiltration, consisting in most places of fresh pumice from the 600-yr Inyo Craters explosions or of andesitic and dacitic colluvium from numerous blocky outcrops of these rocks. As a result, there is little direct runoff, and recharge to the cold groundwater system is plentiful. The mountain is mostly treeless above 2900 m, but heavily forested on its flanks, so water losses to sublimation and evapotranspiration are variables that can only be estimated for the entire area (e.g. Heim, 1991). Sorey et al. (1998) estimated that, of the 1–1.5 m of annual precipitation, about 1 m on average recharges, leading to a calculated groundwater flow of 2.5×10^7 m^3/yr for the entire 25 km^2 area of Mammoth Mountain.

As is typical of many young volcanoes, perennial springs are non-existent on the upper slopes. Groundwater outflow is focused by lava flows or other laterally extensive units into high-discharge springs around the lower flanks of the edifice. For example, the locations of the large springs along Boundary Creek on the southwestern flank of the mountain appear to be controlled in part by the extensive andesite flow down this side (Fig. 1).

Much of the north side of Mammoth Mountain is covered by ski runs. The Dry Creek drainage runs down through the ski area and ends $\sim$20 km from the base of the mountain at the margin of the Long Valley caldera. Dry Creek is normally dry beyond the West Moat. Discharge from the Dry Creek groundwater system is commonly assumed to occur at Big Springs (BS). Groundwater flow from Mammoth Mountain all the way to BS has never been demonstrated, but using available data on hydraulic head gradient, transmissivities, volcanic stratigraphy, and some chemical and isotopic data, Heim (1991) estimated that about 10% of the water discharge at BS could result from precipitation on Mammoth Mountain. The large andesite flow that terminates at the northern caldera margin (Fig. 1) is representative of many buried flows of andesite and basalt, some thought to originate near Mammoth Mountain, that form possible aquifers. The precipitation distribution estimates of Heim (1991) suggest that 75% of the discharge at BS is groundwater from the Dry and Deadman Creek drainages (including the Mammoth Mountain component), and 25% is from the Glass Creek drainage.

Despite recent volcanism and intrusion, there is only one hot spring on Mammoth Mountain, the 47°C Reds Meadow tub (RMT), located at the western base. Just 1–2 km off the western base are two high-TDS soda springs (USC and DPP in Fig. 1).

3. Methods

3.1. Gases

Dissolved [O_2] (where [*i*] indicates 'concentration(s) of *i*') was measured on-site with a standard DO meter and probe. If the springs produced free gas bubbles, these were trapped in an inverted funnel and collected into pre-evacuated Pyrex tubes. Gas samples were analyzed for bulk composition by gas chromatography and for $\delta^{13}C$-CO_2 by mass spectrometry using methods published previously (Evans et al., 1981). For noble gas measurements, bubbles were collected from an inverted funnel directly into 10-cm^3 Cu tubes that were then sealed at both ends with refrigeration clamps. The same 10-cm^3 Cu tubes were used at non-bubbling springs, but were completely filled

with water before sealing. Analytical procedures are those of Kennedy et al. (1985) and Hiyagon and Kennedy (1992).

3.2. pH, alkalinity, [CO_2] and DIC

Many methods of determining the carbonate speciation in natural waters exist. Most investigators measure alkalinity combined with either pH (e.g. Presser and Barnes, 1974), pCO_2 (e.g. Pearson et al., 1978), or DIC (e.g. Kroopnick, 1974). Because CO_2 and DIC were the key parameters of interest in this study, several techniques were used. The pH measurement was made on-site using double-buffer calibration at the temperature of the spring or well. Frequently, two or three meter-and-electrode combinations were used simultaneously to reduce the possibility of erroneous readings. Agreement to within 0.03 pH units was sought and generally obtained. Water for alkalinity was collected in tightly sealed glass bottles. Alkalinities were determined by H_2SO_4 titration at the end of each day of sample collection.

At many sites, samples were collected for direct measurement of DIC. A syringe was used to withdraw 5–50 cm^3 of water from as deep as possible in the spring vent. The water was injected through a septum into a pre-evacuated, pre-weighed 250 cm^3 Pyrex 'DIC tube' equipped with a vacuum stopcock. Immediately, 0.5 ml of 6 M HCl was injected into the sample, converting all the DIC to CO_2 and preserving the sample for storage. In the laboratory, the CO_2 was extracted into a liquid-nitrogen trap on a high-vacuum line. Each DIC tube was repeatedly shaken and extracted until all ($>99\%$) the CO_2 in the sample was collected in the trap. The trap was allowed to thaw, releasing any CO_2 trapped in the ice, before the CO_2 was dried and quantified using a calibrated electronic transducer or a Hg manometer. The DIC value was calculated from the quantity of CO_2 and the weight of water in the DIC tube.

In a few cases, [CO_2] was determined by collecting a sample of water directly into an evacuated Pyrex tube. After equilibration at 25°C, the headspace pressure of each gas species was determined by gas chromatography. Dissolved gas concentrations were then calculated from the gas/water ratio in the sample tube (methods discussed in Evans et al., 1988).

3.3. O, H, and C isotopes

Samples of water for oxygen and hydrogen isotopic analysis were collected in tightly sealed glass bottles. The $\delta^{13}C$-CO_2 in the bubble gases was measured on purified aliquots of the CO_2. The $\delta^{13}C$-DIC and ^{14}C were determined in most cases using purified CO_2 extracted from the DIC tubes. In those cases where no DIC sample was collected, a separate sample of water was immediately preserved in a glass bottle with ammoniacal strontium chloride. Pure, dry CO_2 was obtained from the strontium carbonate precipitate and analyzed following the long-used method described by Gleason et al. (1969). The $\delta^{18}O$, $\delta^{13}C$, and δD analyses were run on Finnigan MAT 251 and delta E mass spectrometers; ^{14}C analyses were run at the CAMS facility at Lawrence Livermore National Laboratory.

3.4. Stream flows and water chemistry

Spring flows were gaged using a pygmy meter following standard USGS procedures (Buchanan and Somers, 1969). At many sites, gaging was repeated in different seasons and years. At some sites, pH was determined at selected locations downstream from the vents and used in conjunction with the gaging to calculate how much CO_2 was being lost to the atmosphere at each stretch of the stream. Filtered (0.45 μm) water samples were collected at many sites for anion analysis by ion chromatography, with a split acidified with HNO_3 for cation analysis by inductively coupled argon plasma spectrophotometry.

4. Results

Some of the analytical results shown in Tables 1–3 have been presented in Sorey et al. (1998; 1999) and Evans et al. (1998), but are repeated here for completeness. Analyses of the gas from bubbling springs are given in Table 1. While CO_2 is a major constituent, the air gases N_2, O_2, and

Table 1
Composition of bubbling gases

Site	Date	He	H_2	Ar	O_2	N_2	CH_4	CO_2
USC	Sep-99	0.0002	0.0003	0.0056	0.0305	0.282	0.0005	100.1
DPP	Sep-99	0.0522	< 0.0002	0.185	0.0376	20.9	0.0023	78.3
SLS	Sep-99	0.0031	0.0006	0.890	14.3	67.0	0.0001	17.2
SJTAT	Aug-97	0.0016	0.0014	0.440	8.33	38.5	0.0005	52.6
LBCN	Aug-98	0.0016	< 0.0002	0.396	8.58	35.2	< 0.0002	55.1
LBCS	Aug-98	0.0016	< 0.0002	0.387	8.40	34.1	< 0.0002	56.4
CH12S	Aug-98	0.0040	< 0.0002	0.247	5.37	24.8	0.0006	69.7
VSS	Aug-97	0.0035	0.0116	0.536	9.81	48.1	< 0.0002	40.6

Values are vol%. Analytical uncertainties are the greater of 1% or 2 ppm. $C_2H_6 < 0.0002$; $H_2S < 0.0005$; and $CO < 0.001$ in all samples.

Ar also make up a large fraction of the gas at most sites. Measured values of temperature, specific conductance, dissolved [O_2], pH, and alkalinity (as HCO_3^-) are shown in Table 2. The range in temperature of the cold springs reflects in part the large range of discharge elevations, from 2750 m for CH12S to 2200 m for BS, but SLS, located near the RMT hot spring, does have an identifiable thermal component. Well discharges are slightly warmer than the springs. Apart from USC and DPP, which have the very high alkalinities generally associated with soda springs, all of the cold waters are dilute (< 750 μS/cm) and most contain substantial dissolved O_2 ($\sim$30–70% of saturation).

The dissolved [CO_2] values were calculated from the pH and alkalinity using the computer code SOLMINEQ88 (Kharaka et al., 1988), which calculates speciation and mineral saturation states. For all these features, [CO_3^{-2}] is very low, and alkalinity is nearly equal to [HCO_3^-], so the molar [DIC] is generally the sum of alkalinity plus [CO_2]. For comparison, the measured [DIC] values obtained from the DIC tubes are also shown in Table 2. The last column in Table 2 gives the pCO_2 calculated from the alkalinity and either the measured [DIC] (whenever possible) or the pH.

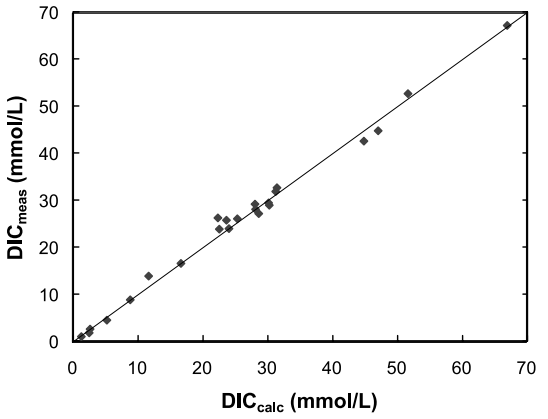

Fig. 2. Comparison of [DIC] calculated from pH and alkalinity with [DIC] values measured in concurrently collected samples.

The calculated and measured [DIC] values are in good agreement (Fig. 2), showing that non-carbonate alkalinity from unidentified sources, such as organic acid anions, is negligible. The measured [DIC] values are preferred in most cases. For example, RMT hot spring forms a pool where CO_2 gas can be lost to the air. Steady CO_2 loss results in a higher pH near the surface, where the pH was measured, than at the submerged inflow point, where the DIC sample was collected. The DIC tube thus gives a higher [DIC] value that more accurately characterizes the fluid. At sites with low [DIC] (< 5 mmol/l), the amount of CO_2 extracted from the DIC tube was too small for accurate manometry, and the calculated [DIC] values should be used. This problem was overcome by collecting a larger aliquot of water in the 1999 sampling of BS.

Table 2 shows that the composition of many of the sites that were sampled on numerous dates did not change much with time. Because of this, the isotopic values from different sampling dates are combined for each site in Table 3. The δD and $\delta^{18}O$ values fit the previously identified regional pattern (Sorey et al., 1993; White et al., 1990). All of the cold waters on Mammoth Mountain

Table 2
Field measurements and DIC speciation

Site	Date	T (°C)	Conductance (μS/cm)	$[O_2]$ (mg/l)	pH	Alkalinity (mmol/l)	$[CO_2]_{(calc)}$ (mmol/l)	$[DIC]_{(calc)}$ (mmol/l)	$[DIC]_{(meas)}$ (mmol/l)	pCO_2 (atm)
Hot and mineralized waters										
RMT	Sep-99	47.0	860	0.3	6.67	8.47	3.17	11.6	13.8	0.251
USC	Sep-99	7.8	2420	0.2	6.11	21.8	45.2	66.9	67.1	0.757
DPP	Sep-99	13.7	2370	0.0	6.08	17.5	34.1	51.6	52.6	0.719
Cold, dilute waters										
RMCS	Aug-96	7.5	227	n.a.	5.48	2.56	25.0	27.6	n.a.	0.418
	Aug-98	7.4	248	4.2	5.41	2.49	28.7	31.2	31.8	0.489
	Jun-99	7.1	246	4.1	5.43	2.51	27.6	30.1	29.4	0.448
	Sep-99	7.3	244	3.7	5.40	2.46	28.9	31.4	32.6	0.503
SLS	Sep-96	18.0	256	n.a.	6.02	2.84	6.30	9.13	n.a.	0.151
	Sep-99	17.7	276	5.2	6.04	2.79	5.99	8.78	8.77	0.139
SJTAT	Aug-97	7.1	272	n.a.	5.56	2.88	23.2	26.1	n.a.	0.388
LBCN	Aug-98	6.8	253	4.6	5.49	2.61	25.4	28.0	29.1	0.427
LBC	Aug-97	7.2	222	n.a.	5.41	2.26	26.0	28.3	n.a.	0.434
	Aug-98	7.0	208	4.4	5.34	2.08	28.1	30.2	28.9	0.447
	Jun-99	7.0	214	4.5	5.37	2.10	26.5	28.6	27.1	0.417
LBCS	Jun-97	6.9	n.a.	n.a.	5.42	2.41	27.8	30.2	n.a.	0.447
	Aug-97	7.8	225	n.a.	5.41	2.28	26.2	28.5	n.a.	0.437
	Aug-98	7.2	224	4.0	5.43	2.34	25.8	28.1	28.0	0.429
	Jun-99	7.0	222	4.5	5.49	2.23	21.3	23.6	25.7	0.392
ASS	Aug-97	6.9	200	n.a.	5.37	2.03	26.3	28.3	n.a.	0.423
	Aug-98	6.2	199	4.6	5.48	2.02	20.2	22.3	26.2	0.389
	Jun-99	7.1	182	4.9	5.44	1.92	20.6	22.5	23.8	0.364
	Sep-99	6.8	201	4.2	5.43	2.06	23.3	25.3	26.0	0.386
CCS	Oct-98	6.8	102	3.0	5.81	1.08	5.16	6.24	n.a.	0.083
MINS	Aug-96	4.1	229	n.a.	7.08	2.29	0.61	2.91	n.a.	0.009
CH12S	Sep-96	2.4	171	n.a.	5.20	1.98	42.6	44.6	n.a.	0.591
	Jun-97	2.4	108	n.a.	5.21	1.44	30.6	32.0	n.a.	0.424
	Aug-97	2.6	206	n.a.	5.17	2.18	49.9	52.1	n.a.	0.692
	Aug-98	2.4	147	3.2	5.07	1.49	43.3	44.8	42.5	0.568
CH12W	Sep-99	3.0	164	2.7	5.06	1.57	45.4	47.0	44.7	0.621
MLS	Aug-96[a]	2.8	284	n.a.	5.59	1.64	14.6	n.a.	16.2	0.196
MMSA1	Aug-96[b]	5.3	229	7.3	5.43	1.79	19.9	21.7	n.a.	0.309
MMSA2B	Aug-96[b]	10.1	372	0.0	5.79	3.44	15.1	18.5	n.a.	0.280
MMSA3	Aug-96	7.3	73	5.4	6.02	0.54	1.56	2.10	n.a.	0.026
DCWELL2	Oct-98	7.8	710	1.8	6.09	7.29	16.8	24.0	23.9	0.277
DCWELL6	Oct-98	7.1	731	5.6	6.41	7.92	8.69	16.6	16.5	0.144
CTRAW	Jun-97	13.0	n.a.	n.a.	7.22	2.15	0.33	2.48	n.a.	0.007
	Aug-98	13.8	246	7.0	n.a.	2.51	n.a.	n.a.	n.a.	n.a.
CTW-2	Aug-98	17.6[c]	148	4.0	8.46	1.21	0.01	1.23	0.96	0.000
BS	Aug-96	11.8	196	n.a.	7.23	1.90	0.30	2.20	n.a.	0.006
	Aug-98	12.3	225	7.3	7.21	2.11	0.34	2.46	1.74	0.007
	Sep-99	12.4	234	7.7	7.14	2.16	0.41	2.58	2.53	0.007
VSS	Aug-97	6.7	278	n.a.	5.44	2.51	27.3	29.8	n.a.	0.440
PDS	Aug-97	11.2	363	n.a.	7.98	3.85	0.11	3.97	n.a.	0.002
TLS	Jul-96	5.3	42	n.a.	6.68	0.43	0.29	0.71	n.a.	0.004
LB-1	Jul-96	5.0	189	n.a.	6.97	1.97	0.66	2.62	n.a.	0.010
CH15S	Sep-96	7.7	381	n.a.	5.94	4.18	13.8	18.0	n.a.	0.231
PSBBC	Oct-98	5.0	294	n.a.	6.70	3.20	1.97	5.16	4.44	0.019
TWIN-In	Sep-97	14.3	38	n.a.	7.83	0.31	0.01	0.32	n.a.	0.000
TWIN-Out	Sep-97	12.8	106	n.a.	7.10	1.02	0.22	1.23	n.a.	0.004

n.a., not measured or not calculable.

[a] DIC measurement based on weight of $SrCO_3$ precipitate; pH calculated from DIC and alkalinity.

[b] $[O_2]$ and $[CO_2]$ from headspace gas chromatography; pH calculated from $[CO_2]$ and alkalinity.

[c] Elevated temperature probably due to solar heating of the discharge pipe.

Table 3
Isotopic data

Site	δD (‰)	$\delta^{18}O$ (‰)	T (TU)	$\delta^{13}C$-DIC (‰)	$\delta^{13}C$-CO_2 ‰	^{14}C (pmC)	$^{3}He/^{4}He$ (R/R_A)
Warm and mineralized waters							
RMT	−108.6[b]	−15.15[b]	n.a.	−5.39[j]	n.a.	8.8[b]	2.2[k]
USC[j]	−111.0	n.a.	n.a.	−3.32	−5.98	n.a.	n.a.
DPP[j]	n.a.	n.a.	n.a.	−4.79	−7.57	n.a.	0.48[k]
Cold, dilute waters							
RMCS	−107.3[g]	−14.88[g]	10.8[b]	−4.83[g], −5.00[j]	n.a.	1.3[b]	3.8[g]
SLS	−104.3[c]	−14.82[c]	9.9[c]	−5.71[j]	−8.44[c]	10.8[c]	3.3[j]
SJTAT[e]	−104.2	−14.74	n.a.	*−6.65*	−5.41	3.0	n.a.
LBCN[g]	−104.7	−14.71	n.a.	−4.59	−4.94	0.6	1.8
LBC	−104.8[g]	−14.83[g]	n.a.	−4.86[i], −4.86[j], −5.05[g]	n.a.	n.a.	3.8[j]
LBCS	−105.2[g]	−14.72[g]	n.a.	−4.79[g], −4.92[i]	−4.84[g]	1.8[d]	4.0[i]
ASS	−106.1[e]	−14.69[e]	13.1[g]	−4.85[i], −4.86[j], −5.00[e]	n.a.	4.3[e]	1.8[g]
CCS[h]	−105.1	n.a.	n.a.	n.a.	n.a.	n.a.	n.a.
MINS[b]	−105.5	−14.93	n.a.	*−11.6*	n.a.	44	n.a.
CH12S	−105.2[d]	−14.76[d]	9.2[c]	−5.07[g], −5.53[e]	−4.88[c], −4.90[e]	2.1[c]	5.0[g]
CH12W[j]	n.a.	n.a.	n.a.	−5.31	−4.79	n.a.	3.8
MLS[b]	−105.2	−14.68	n.a.	*−5.05*	n.a.	2.2	n.a.
MMSA1[b]	−105.6	−14.86	10.1	*−5.87*	n.a.	3.8	4.5
MMSA2B[b]	−109.1	−15.12	14.3	*−7.05*	n.a.	5.1	4.2
MMSA3[b]	−110.0	−15.14	n.a.	*−22.5*	n.a.	112	n.a.
DCWELL2[h]	−108.6	n.a.	16.7	−5.36	n.a.	2.2	n.a.
DCWELL6[h]	−108.4	n.a.	15.1	−5.37	n.a.	4.7	4.2
CTRAW	−111.8[g]	−15.72[g]	12.3[g]	*−7.94*[d]	n.a.	36.5[d]	0.2[g]
CTW-2[g]	−122.9	−16.60	1.4	−13.81	n.a.	70.8	2.7
BS	−115.3[g]	−15.76[g]	9.6[j]	−7.33[j], −7.39[g]	n.a.	41.5[b]	2.3[g]
VSS	−106.6[e]	−14.95[e]	17.8[b]	*−5.90*[b]	−5.57[e]	2.0[e]	3.8[e]
PDS[e]	−107.9	−14.70	n.a.	*−0.35*	n.a.	23.4	n.a.
TLS[a]	−106.8	−14.44	6.5	*−15.9*	n.a.	102	n.a.
LB-1[a]	−107.2	−14.90	11.6	*−9.2*	n.a.	38	n.a.
CH15S[c]	−107.5	−15.16	n.a.	*−9.87*	n.a.	11.3	n.a.
PSBBC[h]	−107.7	n.a.	n.a.	−6.95	n.a.	n.a.	n.a.
TWIN-In[f]	−106.8	n.a.	n.a.	*−6.39*	n.a.	104	n.a.
TWIN-Out[f]	−104.1	n.a.	n.a.	*+1.08*	n.a.	23.6	n.a.

$\delta^{13}C$-DIC values are from DIC-tube sample except those in italics from $SrCO_3$ sample; $\delta^{13}C$-CO_2 from gas bubbles. He isotopic values are corrected for air contamination and are normalized to R_A, the $^{3}He/^{4}He$ ratio in air. n.a., not measured.[a]Jul-96; [b]Aug-96; [c]Sep-96; [d]Jun-97; [e]Aug-97; [f]Sep-97; [g]Aug-98; [h]Oct-98; [i]Jun-99; [j]Sep-99; [k]Pre-1996 from Sorey et al. (1998).

show narrow ranges in both isotopes: −104 to −110 in δD and −14.44 to −15.16 in $\delta^{18}O$. Features such as BS near the northern margin of the caldera are lighter, reflecting a component of precipitation falling east of the Sierran crest. Of the 14 sites where tritium was measured, only CTW-2 contains some pre-1950s water; otherwise, calculated groundwater flow times range from about 1 yr for TLS up to about 30 yr for VSS (Evans et al., 1998).

The $\delta^{13}C$-DIC values obtained from the DIC tubes show excellent reproducibility at sites sampled more than once. For the CO_2-rich waters encountered in this study, this method is probably superior to the $SrCO_3$ method, which allows some gas loss when collection bottles are being filled and preserved.

The $\delta^{13}C$-CO_2 values are given for those features that discharged gas bubbles. Bubbling springs can present a problem for ^{13}C studies because the isotopic fractionation between the gaseous CO_2 and the residual DIC can be substantial. In the temperature range of these features, $\delta^{13}C$-$CO_{2(gas)}$ should be (at equilibrium) 1–1.2 ‰

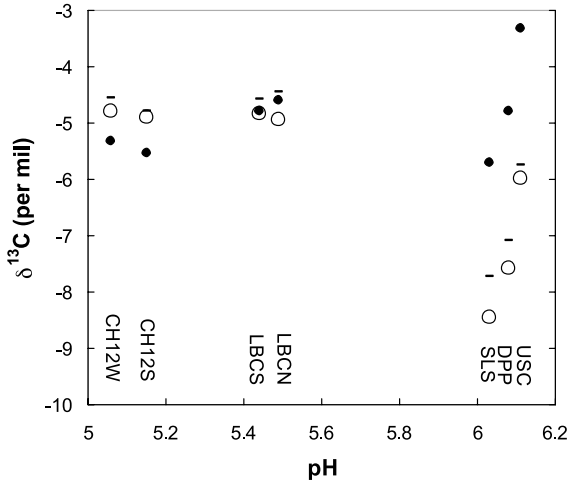

Fig. 3. Sites where both DIC tubes and gas bubble samples were collected. Open circles show measured $\delta^{13}C$-CO_2 in gas bubbles, solid circles show measured $\delta^{13}C$-DIC, dashes show calculated $\delta^{13}C$ values for CO_2 gas in equilibrium with the measured $\delta^{13}C$-DIC.

heavier than $\delta^{13}C$-$CO_{2(aq)}$ and 8–10‰ lighter than $\delta^{13}C$-HCO_3^- (Friedman and O'Neil, 1977). Thus, $\delta^{13}C$ of the $CO_{2(gas)}$ should be lighter than the $\delta^{13}C$ of DIC that is characterized by a $[CO_2]/[HCO_3^-]$ of less than about 8; that is, when pH is above about 5.6. Sites USC, DPP, and SLS show this effect. The $\delta^{13}C$-$CO_{2(gas)}$ is slightly heavier than $\delta^{13}C$-DIC at some of the other features where the $[CO_2]/[HCO_3^-]$ of the DIC exceeds 8, in near agreement with equilibrium fractionation factors (Fig. 3). For all of the features except USC and DPP, the discharge of $CO_{2(gas)}$ is trivial compared to the DIC discharge, and the features are accurately characterized by the $\delta^{13}C$-DIC alone. The best that can be done for USC and DPP without quantifying the gas and liquid discharge rates is to note that their carbon has a $\delta^{13}C$ value somewhere between that of the $CO_{2(gas)}$ and the DIC.

The tritium values show that the cold, dilute groundwaters are not very old, and the ^{14}C depletion thus results from the addition of abiogenic carbon. Many features also show a strong contribution of magmatic helium, similar to that found in the MMF. However, the fumarolic $^3He/^4He$ ratio has not been constant over time, increasing from 3–4 R_A to near 7 R_A just after the 1989 intrusion and then gradually declining back to near 4 R_A over the next decade (Sorey et al., 1998,1999).

Water chemistries are shown in Table 4. The cold, dilute waters have high K/Na ratios, typical of the earliest stage of rock weathering (see Hem, 1985), and their Mg/Na ratios are very high, reflecting the reactivity of mafic minerals in the fresh volcanic rocks. The SiO_2 concentrations are much higher than expected for Sierran cold springs (Feth et al., 1964), with the CO_2-rich features very close to saturation with amorphous silica. Most of these waters are oxygenated, and so Fe and Mn are generally low. The elevated Al in the most acidic waters and the significance of Al mobility at low pH have been discussed by McGee and Gerlach (1998). HCO_3^- is the most abundant anion at all of the features.

Water and carbon discharges of the major features are shown in Table 5. The DIC discharges are calculated using the [DIC] from Table 2, and the discharges of abiogenic or magmatic DIC are calculated using the ^{14}C data from Table 3 (as discussed below).

5. Individual features

5.1. Thermal and mineral springs

The combined water discharge from the thermal and mineral springs RMT, USC, and DPP (Fig. 1) is only a few l/s, and the DIC discharge is small compared to the total from Mammoth Mountain. However, a long sampling history exists for these features (e.g. Barnes et al., 1981; Farrar et al., 1987; Shevenell et al., 1987; White et al., 1990; Sorey et al., 1993). None of these springs has shown notable changes in temperature, chemistry, or isotopic values following the intrusive event in 1989.

The source of heat and volatiles for the 47°C RMT has been discussed by Shevenell et al. (1987) and Sorey et al. (1993), but some uncertainties remain. The water is low in $[O_2]$ and moderately mineralized (Tables 2 and 4) but also contains significant tritium (Shevenell et al., 1987). It may be a relatively young groundwater that

Table 4
Water chemistry[a]

Site	Date	Na (mg/l)	K (mg/l)	Ca (mg/l)	Mg (mg/l)	SiO_2 (mg/l)	Fe (μg/l)	Mn (μg/l)	Sr (μg/l)	Ba (μg/l)	Li (μg/l)	B (μg/l)	Al (μg/l)	Mo (μg/l)	V (μg/l)	F (mg/l)	Cl (mg/l)	SO_4 (mg/l)	NO_3 (μg/l)	Br (μg/l)	PO_4 (μg/l)
Warm and mineralized waters																					
RMT[b]	Sep-99	140	5.7	69	2.3	150	< 3	550	n.a.	n.a.	850	1700	n.a.	n.a.	n.a.	4.1	6.4	30.9	< 10	14	< 20
USC[b]	Sep-99	400	20	130	32	76	n.a.	n.a.	n.a.	n.a.	n.a.	4000	n.a.	n.a.	n.a.	2.2	209	17.5	120	390	< 100
DPP[b]	Sep-99	485	19	43	26	78	2780	350	n.a.	n.a.	2100	7000	n.a.	n.a.	n.a.	2.6	263	31.0	120	440	< 100
Cold, dilute waters																					
RMCS	Aug-96	14.5	7.9	15.0	15.0	81.2	< 2	3	118	21	49	9	< 10	< 2	< 2	0.07	0.28	6.6	< 10	4	130
SLS	Sep-96	32.6	3.2	29.0	3.8	67.0	6	3	298	2	182	262	< 10	7	< 2	1.15	1.14	7.4	< 10	8	< 20
SJTAT	Aug-97	16.3	7.5	17.7	15.0	73.0	< 5	3	153	34	104	25	< 20	< 5	3	< 0.2	0.43	2.9	54	< 20	138
LBCN	Aug-98	14.5	8.0	17.1	12.6	74.5	< 5	5	149	46	94	21	30	< 5	3	0.09	0.45	2.8	81	1	115
LBC	Aug-98	13.6	6.6	13.2	9.7	61.3	< 5	3	116	9	56	19	20	< 5	2	0.12	0.32	3.1	< 10	2	100
LBCS	Aug-98	14.4	6.9	14.9	10.3	66.2	< 5	4	128	16	80	34	50	< 5	2	0.12	0.40	3.2	< 10	3	105
ASS	Aug-98	13.5	6.2	13.6	8.4	59.9	5	2	132	7	54	18	20	< 5	< 2	0.12	0.27	2.9	< 10	3	93
CCS	Oct-98	11.4	1.6	8.0	1.7	35.8	< 5	< 2	61	< 5	31	23	50	< 5	< 2	0.50	0.21	1.1	< 10	3	< 20
MINS	Aug-96	n.a.	n.a.	n.a.	n.a.	n.a.	n.a.	n.a.	n.a.	n.a.	n.a.	n.a.	n.a.	n.a.	n.a.	< 0.05	0.46	8.4	< 10	3	< 20
CH12S	Aug-98	4.3	4.4	19.2	2.4	35.2	< 5	85	112	140	10	< 10	570	< 5	< 2	0.19	0.28	1.3	87	1	< 20
CH12W	Sep-99	n.a.	n.a.	n.a.	n.a.	n.a.	n.a.	n.a.	n.a.	n.a.	n.a.	n.a.	n.a.	n.a.	n.a.	0.27	0.99	6.2	104	< 20	< 20
MLS	Aug-96	n.a.	n.a.	n.a.	n.a.	n.a.	n.a.	n.a.	n.a.	n.a.	n.a.	n.a.	n.a.	n.a.	n.a.	< 0.05	33.3	1.5	4400	6	< 20
MMSA1	Aug-96	15.9	7.7	15.0	10.9	48.3	< 5	163	66	153	54	10	60	< 2	< 2	< 0.05	17.6	4.3	2500	5	< 20
MMSA2B	Aug-96	n.a.	n.a.	n.a.	n.a.	n.a.	n.a.	n.a.	n.a.	n.a.	n.a.	n.a.	n.a.	n.a.	n.a.	0.15	5.7	32.6	1930	3	< 20
MMSA3	Aug-96	n.a.	n.a.	n.a.	n.a.	n.a.	n.a.	n.a.	n.a.	n.a.	n.a.	n.a.	n.a.	n.a.	n.a.	< 0.06	3.4	0.9	1640	6	< 20
DCWELL2	Oct-98	94.4	18.2	19.3	28.1	80.7	423	4	439	50	213	15	< 20	< 5	< 2	0.22	4.2	21.3	1190	2	137
DCWELL6	Oct-98	94.0	16.8	19.7	32.6	72.2	335	9	373	69	157	12	< 20	< 5	6	0.25	2.9	13.1	690	3	159
CTRAW	Aug-98	33.3	5.2	6.0	9.8	64.8	< 5	< 2	53	18	65	149	< 20	9	24	0.48	2.5	6.8	< 10	6	420
CTW-2	Aug-98	15.1	2.7	9.2	3.8	45.9	26	< 2	112	25	< 2	155	< 20	< 5	8	0.25	4.2	7.0	< 10	14	< 20
BS	Aug-98	28.9	5.1	6.2	8.4	60.8	< 5	< 2	64	20	47	253	< 20	7	20	0.44	5.0	6.7	133	13	390
VSS	Aug-96	21.7	3.5	18.2	17.4	75.3	< 2	2	65	6	106	5	< 10	< 2	< 2	0.13	0.46	18.1	< 10	5	330
PDS	Aug-97	33.1	5.3	14.5	21.7	73.8	170	239	101	7	104	20	< 20	< 5	< 2	0.37	0.23	6.6	< 10	< 20	53
TLS	Jul-96	n.a.	n.a.	n.a.	n.a.	n.a.	n.a.	n.a.	n.a.	n.a.	n.a.	n.a.	n.a.	n.a.	n.a.	< 0.05	0.40	1.9	< 10	3	< 20
CH15S	Sep-96	18.8	8.8	48.8	12.4	72.4	8800	3200	224	82	48	14	80	< 2	< 2	0.10	1.08	8.8	< 10	9	< 20
PSBBC	Oct-98	19.3	7.0	13.6	19.3	40.8	< 5	< 2	135	14	6	15	< 20	< 5	6	0.09	0.69	0.2	39	< 20	130
TWIN-In	Sep-97	1.3	0.4	6.0	0.2	3.6	19	< 2	15	< 5	< 2	< 10	< 20	6	< 2	< 0.05	0.08	3.2	< 10	2	< 20
TWIN-Out	Sep-97	4.0	1.6	12.0	3.8	7.3	131	15	46	9	7	< 10	< 20	< 5	< 2	0.18	0.23	3.4	< 10	5	31

NO_3 reported as N; PO_4 reported as P. n.a., not measured.

[a] Analytical uncertainties are generally 5%, but precision and detection limits vary from sample to sample according to specific analytical conditions.

[b] Cations, SiO_2, and B from Farrar et al. (1985).

has been steam-heated, or may have circulated through a shallow region where the rock retains some heat from previous intrusions. The δ^{13}C-DIC value of −6.0‰ and ^{3}He/^{4}He of 2.6 R_A (Table 3) demonstrate a magmatic gas component.

Soda springs USC and DPP discharge small amounts of mineralized, Fe-rich fluid at the edge of the San Joaquin River and are seasonally underwater. The recharge area for these springs is unclear as they discharge through older rocks off the Mammoth Mountain edifice. The gas in these springs could be sourced beneath Mammoth Mountain, but the ^{3}He/^{4}He at DPP is low, 0.48 R_A, and similar high-TDS soda springs are scattered throughout the Sierra Nevadan batholith with no clear tie to volcanics.

Barnes et al. (1981) argued that the high Mg^{2+}, Cl^-, Br^-, I^- concentrations and ^{87}Sr/^{86}Sr ratios in the suite of Sierran soda springs reflected reaction with ultramafic and meta-sedimentary rocks deep beneath the Sierran granite. The global correlation between this type of CO_2-rich spring and areas of seismic activity established by Barnes and his colleagues (e.g. Barnes et al., 1984) strongly supports the concept of deep circulation along faults. Such fluids all tap some deep source of CO_2 that is then substantially neutralized by water–rock interactions, increasing the TDS of the fluid. In individual cases, the question of whether this CO_2 source is the mantle, magmatic degassing, or thermal metamorphism of carbonate rocks (e.g. in basement or roof pendants) is as unsettled as it was in the time of Barnes' studies.

5.2. Cold, dilute springs and wells

Some of the cold, dilute waters on Mammoth Mountain have been sampled in previous studies, but the major role that these groundwaters play in magmatic carbon transport was not realized until several years after the forest die-off, when our sampling focused on [CO_2] and DIC.

5.2.1. Reds Creek area

The RMCS spring group forms the headwaters of the perennial part of Reds Creek, and the outflow stream passes within 2 m of the hot spring RMT. Despite the fact that the DIC discharge from RMCS dwarfs that from the hot spring, our sampling of the RMCS spring vent in 1996 was the first revelation of the huge DIC component in the Mammoth Mountain cold springs. The SLS spring group produces weakly thermal water that may contain a component of RMT-type fluid to account for its low K/Na and Mg/Na ratios and the high [F] and [B] relative to the other springs. SJTAT is representative of several low-flow, widely spaced springs between Reds Creek and Boundary Creek, all of which issue near the 2500-m elevation contour.

5.2.2. Boundary Creek area

LBCN, LBC, LBCS, and ASS are all high-flow features that issue in close proximity. CCS is a low-flow seep with a slightly elevated [DIC] that marks the southernmost extent of the DIC anomaly. It is chemically distinct from the nearby LBC and ASS springs in having low K/Na, Mg/Na, and [PO_4^{-3}], and elevated [F^-], and probably consists mainly of groundwater draining the granitic ridge to the southeast of Mammoth Mountain (Fig. 1).

5.2.3. Dry Creek area

The low-discharge MINS is only slightly enriched in DIC but contains some abiogenic carbon (Table 3). Less than 1 km to the SE, the high-discharge CH12S spring issues in close proximity to the CH12 tree-kill area (Sorey et al., 1998), and a well (CH12W) drilled nearby in 1999 encountered similar DIC-rich water at ~30 m depth.

MLS is a small ephemeral spring that flows only for a short period following snow melt and issues a few meters away from the main ski lodge. MMSA1 (37 m deep) and MMSA2B (100 m deep) are pumped wells, and MMSA3 is either a shallow artesian well or spring that fills a concrete tank. The wells supply water that is used for snow-making at the ski area. These DIC-rich features all show a clear signature of the NaCl and NH_4NO_3 salts that are spread onto the snow in large quantities to improve skiing (Table 4). Snowmelt from the ski area contributes a Cl^- and NO_3^- anomaly to the groundwater.

DCWELL2 and DCWELL6 are water-supply

wells drilled in the late 1980s but currently unused. CTRAW, 2 km up-gradient from BS, is a 100-m-deep well that supplies water to a roadside rest area. CTW-2 is a 100-m-deep well tapping groundwater from the northwest rim of the caldera in the Glass Creek drainage. BS forms the headwaters of the Owens River, discharging through many orifices spread over hundreds of meters of channel.

5.2.4. Lakes basin and Mammoth Creek area

VSS is the only high-flow spring in this area. PDS, on the south side of Mammoth Creek, may not contain any water from Mammoth Mountain. TLS, a dilute spring with a slightly heavy $\delta^{18}O$, may contain subsurface leakage from one of the lakes up-gradient. LB-1 is a small water-supply well for local cabins. CH15S is one of the few dilute springs that is anoxic and iron-rich.

PSBBC flows from a driven pipe in an area of groundwater seepage near the shore and beneath the surface of Twin Lakes. The total seepage here is sufficient to alter the chemical and isotopic characteristics of the lake water, as can be seen by comparing the inlet (TWIN-In) and outlet (TWIN-Out) values (Tables 2–4). TWIN-In has a water chemistry reflecting the granitic rock in the catchment, for example, a low [Mg]/[Na] and

Table 5
Flow data (DIC in t/day as CO_2; italicized values are approximated using an inferred [DIC])

Site	Date	Water flow (l/s)	Total DIC flow (t/day)	Magmatic[a] DIC flow (t/day)
LBC[b]	Aug-97	48	*5.16*	5.11
LBC[b]	Aug-98	282	31.0	30.7
LBC[b]	Jun-99	132	13.6	13.5
LBC[b]	Jul-99	205	*21.8*	21.6
LBC[b]	Sep-99	42	*4.47*	4.43
LBCS	Aug-97	54	5.85	5.76
LBCS	Aug-98	124	13.2	13.0
LBCS	Jun-99	79	7.72	7.60
LBCS	Jul-99	104	*10.7*	10.5
LBCS	Sep-99	49	*5.03*	4.95
ASS	Aug-97	41	4.41	4.23
ASS	Aug-98	107	10.7	10.2
ASS	Jun-99	65	5.88	5.65
ASS	Jul-99	66	*6.52*	6.26
ASS	Sep-99	33	3.26	3.13
RMCS	Aug-97	75	*8.72*	8.38
RMCS	Aug-98	161	19.5	19.3
RMCS	Jun-99	83	9.28	9.18
RMCS	Jul-99	109	*12.7*	12.6
RMCS	Sep-99	54	*6.28*	6.22
CH12S	Aug-97	37	7.33	7.18
CH12S	Aug-98	30[c]	4.85	4.75
CH12S	Jul-99	22	*3.96*	3.88
SLS	Sep-99	29	0.97	0.88
BS	Sep-99	1050[d]	10.1	6.51
SJTAT	Aug-97	15[e]	1.49	1.44
VSS	Aug-97	10[c]	1.13	1.10
TWIN-Out	Sep-97	203[f]	0.95	0.76

[a] Actually, abiogenic DIC flow (see text).
[b] Includes flow from LBCN.
[c] Visually estimated flows.
[d] Total discharge, 10% of which is thought to be from Mammoth Mountain (see text).
[e] Total estimated flow of several springs.
[f] Flow of Mammoth Creek containing some groundwater from Mammoth Mountain (see text).

[Cl^-]. TWIN-Out is enriched in [Mg]/[Na] and heavily depleted in ^{14}C. In both these surface waters, [SiO_2] is reduced due to diatom growth. The in-seepage of high-DIC fluid causes the pCO_2 of the lake water (e.g. TWIN-Out) to be greater than in air. Loss of CO_2 from the lake surface therefore causes our estimate of the magmatic DIC discharge from seepage (Table 5) to be somewhat low.

6. Discussion

6.1. CO_2 and weathering

Some fraction of the CO_2 gas absorbed by groundwater is involved in water–rock interaction or weathering. These processes are complex, but can be viewed in simplest terms as a mechanism of neutralizing fluid acidity and converting dissolved CO_2 to HCO_3^- (and CO_3^{-2}). The most important types of reactions to consider in volcanic terranes are silicate hydrolysis reactions; for example,

$$2CO_2 + 3H_2O + 2NaAlSi_3O_8 = Al_2Si_2O_5(OH)_4 + 2Na^+ + 4SiO_2 + 2HCO_3^- \quad (1)$$

$$4CO_2 + 2H_2O + Mg_2SiO_4 = 2Mg^{2+} + SiO_2 + 4HCO_3^- \quad (2)$$

with other silicate minerals contributing K^+ and Ca^{2+} in similar fashion. In the initial stage of CO_2-weathering, the major cations are released to solution in ratios similar to those of the rock (see e.g. Giggenbach, 1988). In these reactions, molar DIC and $\delta^{13}C$-DIC are conserved as CO_2 converts to HCO_3^-. However, the rising pH can eventually create enough CO_3^{-2} to form mineral precipitates with Ca^{2+}, Mg^{2+}, and Fe^{2+}, thus reducing the DIC of the water. Most of the Mammoth Mountain waters are still acidic and oxic (Table 2), and likely have not deposited much carbonate. None show saturation with siderite, and only RMT is at saturation with calcite.

Marine carbonate rocks are not present within the volcanic edifice, but flow through underlying meta-sedimentary rocks that contain carbonate minerals may impact some of the distal features. Carbonate minerals contribute to the HCO_3^- through:

$$CO_2 + H_2O + CaCO_3 = Ca^{2+} + 2HCO_3^- \quad (3)$$

The molar DIC increases two-fold in this reaction, and the $\delta^{13}C$-DIC value reflects a mixture of the carbon sources. Natural waters can have many sources of acidity other than CO_2, all of which can release HCO_3^- from carbonate minerals.

In complex situations involving many different sources and sinks for carbon, geochemical and flow-path modeling can frequently identify the most important processes that influence a given suite of groundwaters (for a recent example, see (Chiodini et al., 2000). In any case, while soil-gas studies focus on CO_2 flux, groundwater studies must consider DIC.

6.2. Gas sources

In the model recently proposed by Sorey et al. (1998), a large reservoir of high-pressure gas is trapped beneath a low-permeability seal within Mammoth Mountain. The 1989 intrusion served both to provide a fresh pulse of magmatic gas and to breach the low-permeability seal, releasing the trapped gas. Some of the trapped CO_2 could actually derive from thermal destruction of deeply buried carbonate rocks but will be referred to here as 'magmatic'. In any case, the $\delta^{13}C$ value in steam vent Mammoth Mountain fumarole (MMF) changed $< 1‰$ following the intrusion and has remained at $-5 \pm 0.5‰$ over the entire period of record (1982 to the present). The $\delta^{13}C$ values in soil gas in all the tree-kill areas are also close to $-5‰$. This constancy in $\delta^{13}C$ means that groundwaters highly enriched in magmatic CO_2 should have a $\delta^{13}C$-DIC near $-5‰$ regardless of the year or precise location of recharge.

All groundwaters acquire some biogenic CO_2, particularly during infiltration through vegetated soils. Biogenic CO_2 is produced by several processes, and the $\delta^{13}C$ and ^{14}C values are not as

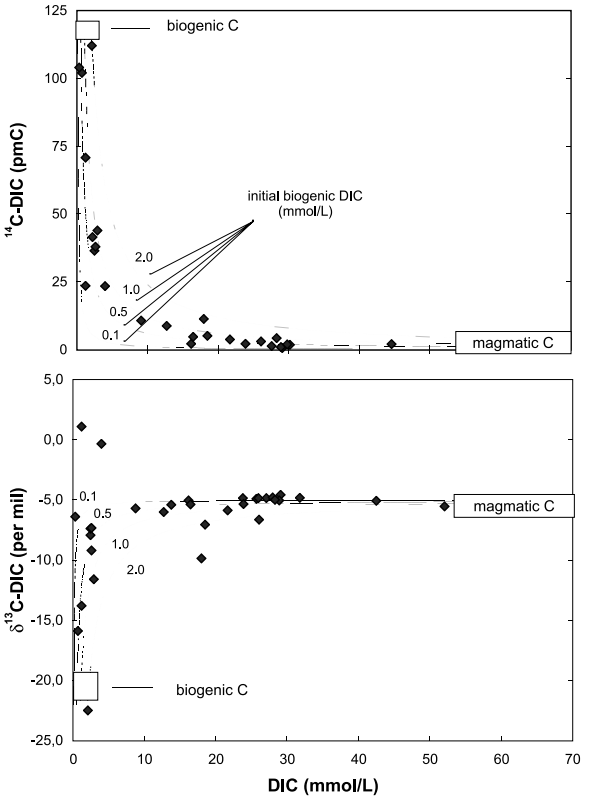

Fig. 4. The $\delta^{13}C$ and ^{14}C vs. the [DIC] on same date of collection (after Chiodini et al., 2000).

tightly constrained as for the magmatic end member. Plant-root respiration, probably the major contributor in these soils, produces CO_2 with a ^{14}C content near that of atmospheric CO_2 (110 pmC in 1999). Several soil-gas samples have indicated that the biogenic CO_2 in the forest soils has a $\delta^{13}C$ near $-20‰$ (Sorey et al., 1998). This seems reasonable for root respiration because biogenic soil CO_2 is typically 4–5‰ heavier than the plant biomass (Cerling et al., 1991), and the carbon in wood samples from the local trees averages about $-25‰$ (Cook et al., 2001).

In a study of large aquifers in central Italy, Chiodini et al. (2000) used plots of [DIC] vs. $\delta^{13}C$ to trace the addition of deep carbon to groundwaters containing biogenic carbon from infiltration. The Mammoth Mountain data is presented in an analogous plot in Fig. 4. These plots clearly show the dependence of the isotopic evolution on the initial concentration of biogenic carbon. Groundwaters only slightly enriched in magmatic carbon can show a wide range of isotopic values, but at higher [DIC], the isotopic composition of the magmatic end member is clearly indicated.

The ^{13}C–^{14}C plot in Fig. 5 eliminates concentration and compares the data to a mixing line. Of the plotted sites, CTW-2 in the Glass Creek drainage receives no water from Mammoth Mountain. PDS is thought to receive some flow from areas of carbonate rocks (Fig. 1), a possibility supported by its heavy $\delta^{13}C$ value. The Twin Lake samples are obviously influenced by open-system CO_2 exchange with the atmosphere, which fractionates the $\delta^{13}C$ values. Other samples plot on a fairly linear trend, and a regression line through these points gives the magmatic end member a $\delta^{13}C$ value of $-5.0‰$ at 0 pmC, identical to the values of the fumarolic CO_2 at MMF. The line is not well-constrained at high ^{14}C values, but passes near the composition assigned to present-day biogenic soil CO_2. If we take $-20‰$ as the best estimate of the $\delta^{13}C$ value of biogenic DIC expected in infiltrating groundwaters, then the regression line gives a ^{14}C of 117 pmC. It is reasonable for the biogenic DIC in groundwaters recharged between 1 and 30 yr ago to contain slightly more ^{14}C than the present-day soil gas CO_2 (110 pmC), because the ^{14}C content of atmo-

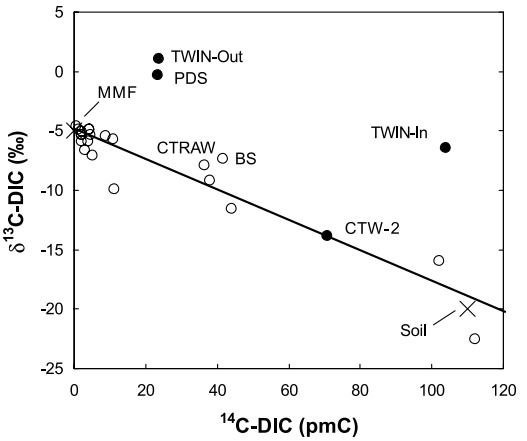

Fig. 5. The $\delta^{13}C$ vs. ^{14}C in the DIC. Filled symbols indicate points not used in calculating the regression line shown.

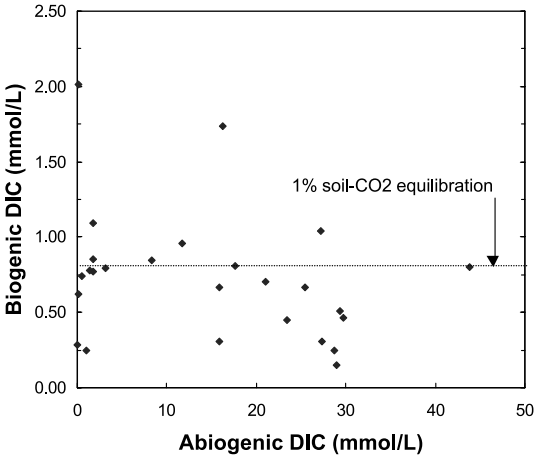

Fig. 6. Division of DIC in each feature into biogenic and abiogenic fractions based on a biogenic end member ^{14}C of 117 pmC. Dotted line shows calculated biogenic [DIC] in snowmelt infiltrating soil with a [CO_2] of 1% from soil respiration.

spheric CO_2 has changed from 155 to 110 pmC during that time (see Cook et al., 2001).

Assuming 117 pmC to represent the biogenic end member for all the dilute waters, then the ratio of the ^{14}C values in Table 3 to 117 gives the biogenic fraction of the DIC for each individual feature. Multiplying this by the [DIC] in Table 2 gives the concentration of biogenic carbon, which for all the sites, falls in the narrow range of 0.15–2.0 mmol/l, as shown in Fig. 6. These biogenic DIC concentrations are consistent with groundwater recharge as snowmelt through soils containing $\sim$0.3–3% biogenic CO_2, similar to the range found in gas samples from the healthy forest soils (Evans et al., 1998). The remainder of the [DIC] is abiogenic and varies greatly among the sites, from 0 to 51 mmol/l. There is no significant inverse correlation between biogenic and abiogenic DIC, as would be expected if waters that had acquired large amounts of abiogenic CO_2 then lost a substantial amount of CO_2 prior to discharge. This, and the linear trend in Fig. 5, argues for closed-system behavior during flow. The groundwaters retain any CO_2 they acquire until depressurization at the vent allows bubbles to begin to form.

The main goal of our study is to quantify the magmatic CO_2 that is absorbed and transported in the cold groundwater system. For all the features listed in Table 5, except BS, the only reasonable source of the abiogenic DIC is the magmatic gas beneath Mammoth Mountain. Multiplying the concentration of abiogenic DIC in each feature by its water flow thus gives the discharge of magmatic DIC.

6.3. The Big Springs question

While the abiogenic carbon in the springs located on the volcano has only one obvious source, this is not the case for BS (Fig. 1), located at a distance and discharging water from many different recharge areas. The carbon in BS raises questions that are not unique to Mammoth Mountain. As more studies look at high-discharge springs in volcanic regions, but not necessarily on volcanoes (Rose and Davisson, 1996; James et al., 1999; Chiodini et al., 2000), identifying carbon sources becomes a major issue. Identifying the source(s) of abiogenic carbon in BS is important because the discharge is substantial (6.5 t/day) and because the ^{14}C record in ancient aquatic vegetation downstream in the Owens River suggests that BS

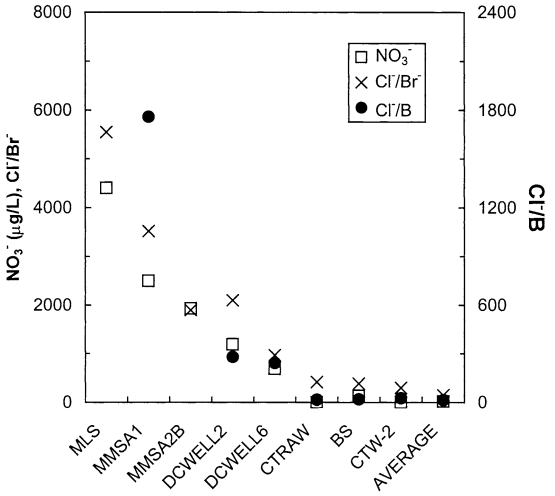

Fig. 7. Effects of salts (NaCl and NH_4NO_3) from ski runs on groundwater draining Mammoth Mountain to the northeast down the Dry Creek drainage (NO_3^- in µg/l). 'Average' values were calculated from the cold springs in Table 4 that are not part of the Dry Creek drainage.

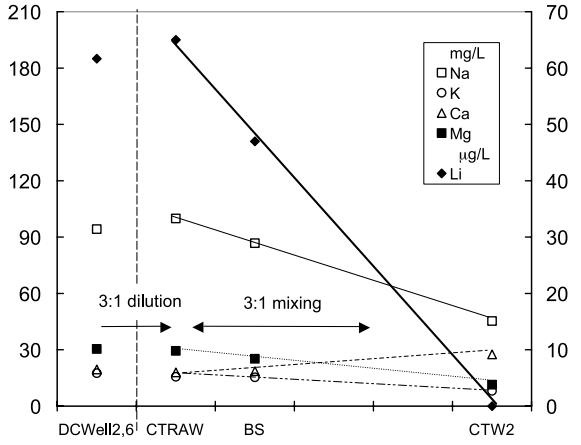

Fig. 8. Major cations that suggest connection between DCWELL2, 6 and CTRAW, both of which show Na > K+ Ca+Mg. Vertical scale change between DCWELLS and CTRAW indicates dilution. Mixing lines shown between CTRAW and CTW-2 pass through BS at a 3:1 ratio.

was discharging abiogenic carbon 600 yr ago (Reid et al., 1998).

Geochemical tracing of the flows of water and DIC to BS is the focus of a separate report (Evans et al., 2001), summarized here, that strongly supports the hydrologic modeling of Heim (1991). The anion data show that ski-run salts (NaCl and NH_4NO_3), which are conspicuous in waters on the north side of Mammoth Mountain, are clearly detectable in the DCWELL samples (Fig. 7). High $[NO_3^-]$, $[Cl^-]/[Br^-] > 1000$, and $[Cl^-]/[B] > 200$ are inconsistent with simple rock weathering and demonstrate groundwater flow from Mammoth Mountain down the Dry Creek drainage. Ski-run salts are not detectable at CTRAW, but this may reflect a long flow time to this site. Continued monitoring for these unique tracers at all the wells and springs along the Dry Creek drainage is clearly warranted.

The cation data in particular suggest that groundwater from the DCWELL area eventually reaches CTRAW, diluted by a factor of 3 from precipitation that infiltrates in the West Moat and inflow from the Deadman Creek drainage (Fig. 8). 'In addition, the 3:1 mixing of this Dry/Deadman Creek groundwater (CTRAW) with Glass Creek groundwater (CTW-2), proposed by Heim (1991) for the BS discharge is strongly supported...' by virtually every chemical and isotopic constituent measured, apart from B and Cl^- (Table 4). The Paleozoic meta-sediments exposed nearby (Fig. 1) are the most probable source for the additional B and Cl^- in BS (see Shevenell et al., 1987), but these rocks are apparently not a significant source of abiogenic carbon. A 3:1 mix of CTRAW and CTW-2 (Tables 2 and 3) would have a ^{14}C of 41.3 pmC, very near the 41.5 pmC observed at BS (Table 3).

The elevated $^3He/^4He$ ratio at BS was initially thought to derive from Mammoth Mountain. However, the low ratio subsequently obtained from CTRAW and the high $^3He/^4He$ ratio and high total [He] from CTW-2 (each well sampled twice), show that the magmatic He in BS derives instead from the Glass Creek area. A possible gas source in the Inyo domes area and regional CO_2 flux anomalies from soils found by Gerlach et al. (1996) may be related. Assuming that CTW-2 fluid makes up 25% of the water discharge of BS, it would contribute 0.5 t/day of the magmatic DIC based on its ^{14}C and [DIC] values.

Groundwaters draining Mammoth Mountain absorb very little total He because of its low solubility and the shallow depth of the gas–water interaction (Evans et al., 1998). For example, the [He] in MMSA-1 and 2B is only 4–5 times the value in air-saturated water, and at DCWELL2, [He] is low enough to preclude isotopic analysis. The $^3He/^4He$ in groundwater flowing away from the mountain should drop fairly quickly due to the natural ingrowth of ^4He from α-decay or to mixing with ^4He-rich groundwaters draining older terranes, explaining the low $^3He/^4He$ ratio at CTRAW. Still, 6 t/day of magmatic DIC in BS can be attributed to Mammoth Mountain at the present time, even if the ^{14}C depletion 600 yr ago (Reid et al., 1998) was due entirely to Glass Creek inputs.

6.4. Seasonal and long-term variations

The DIC concentrations at individual features show much smaller seasonal variations (Tables 2 and 3) than do the water flows (Table 5). For features where simultaneous gaging and chemistry have been done more than once, there is no evi-

dence that increased water discharge results in dilution of the DIC (Fig. 9). This makes sense in view of the current situation where so much gas is venting through large areas spread around the mountain that the water itself, and not the gas, is the limited constituent. In consequence, the magmatic DIC discharge varies mainly with water flow.

Water flow variations probably reflect the annual snowfall and timing of snowmelt, which in some years can peak well into summer. The stream gaging was done in summer or fall and may not be representative of conditions in winter, when many of the sites are inaccessible. Some features (e.g. BS, RMT, RMCS) are known to maintain good flows throughout the winter. The outflow channel from CH12S has been dry when observed through snow pits, but the nearby ski-area wells are pumped at higher rates during the early winter for snow-making, possibly offsetting the change in spring discharge.

The average water flow measured from all the features in Table 5 totals 570 l/s, or 1.8×10^7 m^3/yr. This total includes the 10% of the BS water discharge thought to derive from Mammoth Mountain, but not the Twin Lakes seepage and all the low-discharge features, which would raise the total slightly. The total measured flow is reasonably close to the estimated recharge for the entire mountain of 2.5×10^7 m^3/yr (Sorey et al., 1998), suggesting that our groundwater sampling program was fairly complete and that our summer–fall water discharge may fairly represent the annual average.

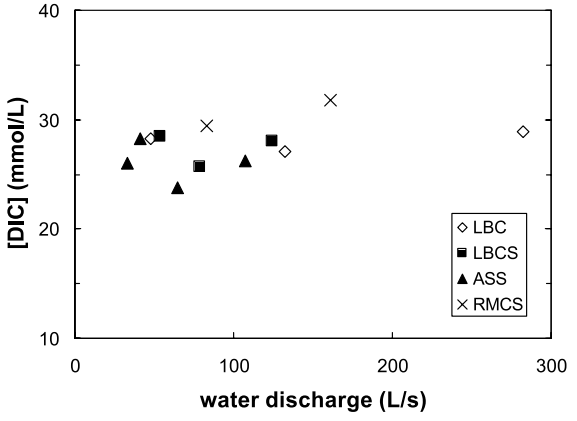

Fig. 9. [DIC] vs. discharge at selected sites.

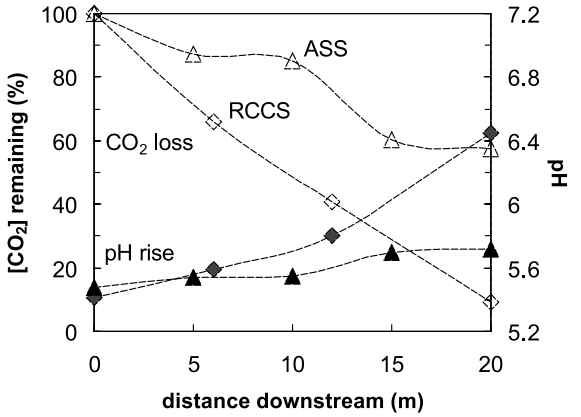

Fig. 10. Rate of CO_2 loss from outflow streams at ASS and RCCS determined from downstream pH measurements in August 1998. These data show ASS losing 3.4 t/day and RCCS losing 15.5 t/day of mainly magmatic carbon in first 20 m of flow, near where tree cores were collected.

Sorey et al. (1998) reviewed the somewhat limited evidence for magmatic carbon discharge in groundwater in the years prior to the 1989 intrusion. The VSS spring was gassy in the early 1950s, and MMSA1 and 2 have produced CO_2-rich water from the time that they were drilled in 1958 and 1982, respectively. Farrar et al. (1985, 1987), report δ^{13}C-DIC of -12.3‰ for MINS and -8.8‰ for BS, indicating that these waters contained magmatic carbon in the early 1980s. Cook et al. (2001) recently presented compelling evidence that two of the larger springs had substantial discharges of magmatic DIC before 1989. Cores or sections were collected from small trees (1–3 m tall) that overhang the outflow streams of RMCS and ASS and analyzed for ^{14}C in individual growth rings. These springs lose magmatic CO_2 at a rate fast enough to lower the ^{14}C content in the atmosphere around the trees (Fig. 10). Wood produced by the trees is similarly ^{14}C-depleted, providing an annual record of magmatic CO_2 discharge. The tree-ring records show ^{14}C depletion back in time to the birth of the trees, in the mid-1960s at RMCS and mid-1980s at ASS, demonstrating that these springs have been discharging magmatic CO_2 well before the dike intrusion.

Some evidence suggests that the magmatic DIC discharge has increased following the intrusion. The same tree-ring data indicates that the magmatic CO_2 discharge at RMCS and ASS increased in the early 1990s, but the picture is complicated because the increase coincides with the end of a multi-year drought, when water flows were likely to have changed (Cook et al., 2001). Excluding the drought years, the tree-ring data suggest that magmatic CO_2 output might have doubled following the intrusion. Heim (1991) reported partial analyses from several features in the Dry Creek area. At MMSA1, DCWELL2, and DCWELL6, our alkalinities are about 70% greater than either the values of Heim (1991) or some 1989 values in unpublished records of the local water district. These increases in alkalinity most likely reflect increased CO_2 in the waters after the intrusion, leading to more HCO_3^- through silicate weathering. These Dry Creek sites suggest that the increase in magmatic DIC discharge shown by the tree-ring data may have been mountain-wide.

6.5. Total magmatic DIC discharge

The total discharge of magmatic DIC in cold groundwater can be estimated by summing the values in Table 5, using 6 t/day for BS to exclude the Glass Creek contribution. The large seasonal variations in the stream flows complicate the calculation because the features were not all gaged on the same dates. If we use the seasonal flow data at sites gaged many times and assume that the flows at all other sites remain constant, the total discharge of magmatic DIC (as CO_2) ranges from about 32 t/day in September 1999 to 88 t/day in August 1998. The average is 55 t/day, giving an annual discharge of 20 000 t/yr. All the other springs not shown in Table 5 probably combine for a few additional t/day at most.

The total discharge of magmatic DIC is several times smaller than the combined soil efflux of magmatic CO_2 from all of the tree-kill areas, most recently estimated at 200–300 t/day (Sorey et al., 1999; Gerlach et al., 1999), but is about half as large as the efflux from the large, well-studied Horseshoe Lake tree-kill area. Significantly, it is one to two orders of magnitude larger than the focused CO_2 discharge from steam vents. MMF, by far the most vigorous vent, currently emits 1 t/day of CO_2, with vents in the other two fumarolic areas emitting significantly less than this (Sorey et al., 1993). Unlike the CO_2 released to the atmosphere, the magmatic CO_2 transported in the groundwater system is directly involved in weathering of the Mammoth Mountain edifice. Using the water flows (Table 5) and the cation chemistry (Table 4) in equations like Eqs. 1 and 2 indicates that $\sim$10 000 t/yr of silicate minerals are altered during the conversion of CO_2 to HCO_3^-.

Allowing that the DIC flux might have doubled after the intrusion would still put an estimate of the pre-1989 discharge at 10 000 t/yr. In the long term, such a discharge would require an intrusion rate of 0.057 km^3 per century, assuming complete degassing of magma with 0.65 wt% CO_2 and a density of 2.7 t/m^3. This rate is equivalent to at least one intrusion comparable in size to the 1989 event (0.01–0.04 km^3) every 100 yr.

6.6. Lassen cold springs

The findings at Mammoth Mountain raised interest in Lassen volcano, 400 km to the northwest and last active during 1914–1917. Lassen supports

Table 6
Flow and DIC data for Lassen springs

Site	T (°C)	pH	Flow (l/s)	Alkalinity (mmol/l)	[DIC] (mmol/l)	δ^{13}C-DIC	^{14}C (pmC)	Magmatic DIC flow (t/day)
MMFS	4.1	5.60	79	1.95	17.4	−8.66	1.5	5.2
MTS	4.5	6.01	32	1.75	7.27	−10.83	n.a.	0.9[a]
EBMC	9.4	5.63	15[b]	1.97	14.6	−8.61	2.7	0.8

[a] Using δ^{13}C to estimate the magmatic fraction of the DIC as 0.8.
[b] Visually estimated flow.

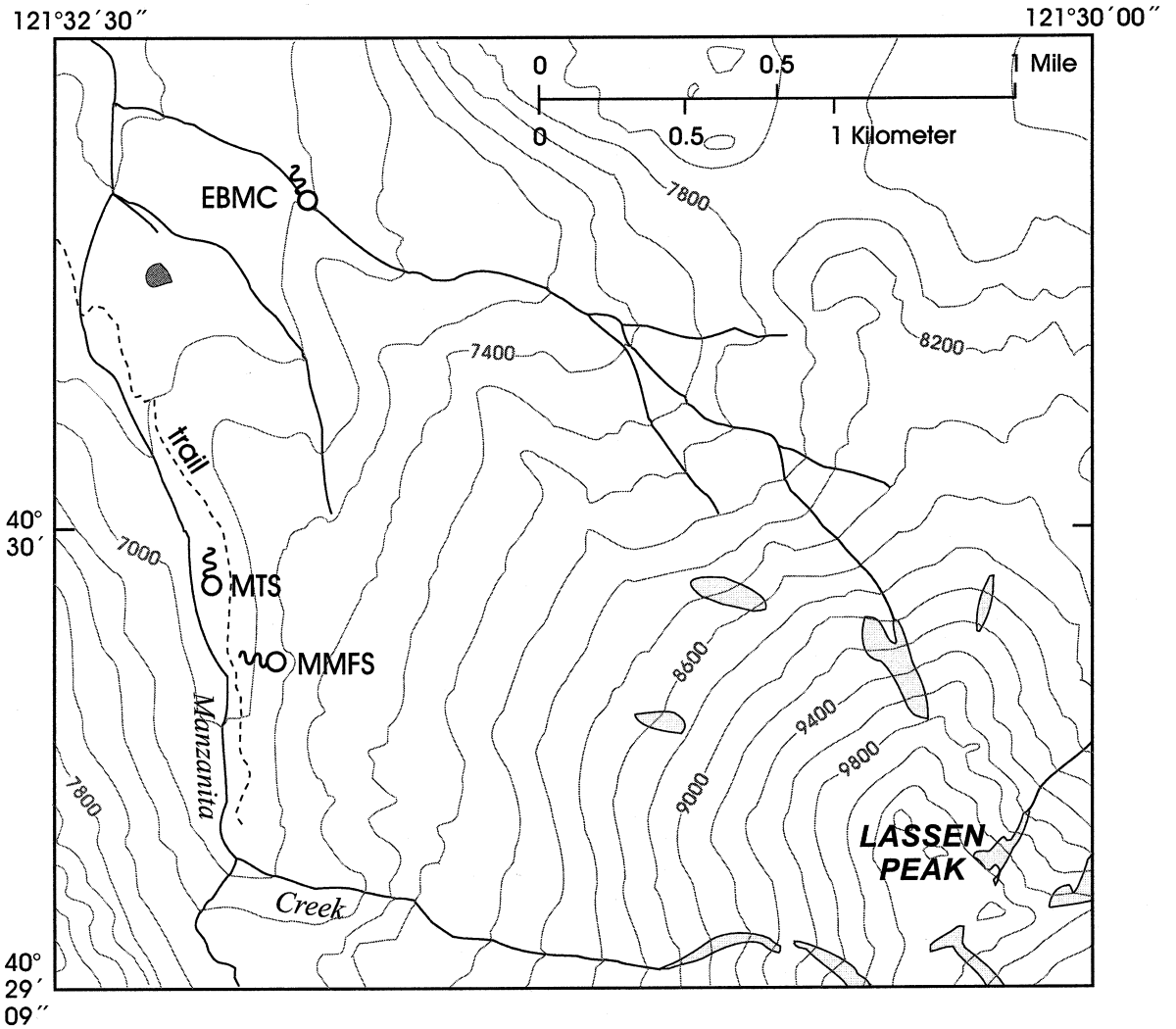

Fig. 11. Newly discovered CO_2-rich cold springs at Lassen volcano.

a large geothermal system that discharges on the southern flanks, but Rose et al. (1996) and Rose and Davisson (1996) recently used ^{13}C–^{14}C data to quantify a sizeable component of magmatic DIC (21 t/day as CO_2) in the cold groundwater system draining the north flanks of the mountain, an area nearly devoid of thermal vents. These studies demonstrated the importance of analyzing cold groundwaters for magmatic CO_2 in locations where the gas is apparently spread over a wide area of diffuse up-flow.

Rose and Davisson (1996) derived the high DIC discharge based on a few high-flow springs, most producing >1000 l/s, with near-neutral pH, [HCO_3^-] near 1 mmol/l, and little CO_2. Our reconnaissance sampling at Lassen in 1998 uncovered three low-pH, high-DIC cold springs (Fig. 11), strongly resembling the features found on Mammoth Mountain. The water flow from all the springs is just over 100 l/s, but they combine for about 7 t/day of magmatic DIC, mainly in the form of dissolved CO_2 (Table 6). Adding this to the estimate of Rose and Davisson (1996) brings the total magmatic DIC discharge to near 28

t/day or 10 000 t/yr, equal to our estimate of the long-term (pre-1989) discharge at Mammoth Mountain. More cold springs at Lassen remain to be studied, and James et al. (1999) have recently reported a magmatic DIC discharge of $\sim 3\times10^4$ t/yr in cold springs draining a 75-km section of the Cascade volcanic arc, a few hundred kilometers north of Lassen.

6.7. Global implications

DIC discharges of $\sim 10^4$ t/yr would have to be common to contribute a significant fraction of the subaerial carbon discharge from volcanoes, a part of the global carbon budget that controls the weathering rates of silicate minerals. However, Chiodini et al. (2000) have recently estimated that cold groundwaters in the volcanic region of central Italy transport between 10^6 and 10^7 t/yr (as CO_2) of deep, probably mantle-derived carbon. Furthermore, the young Mt. Etna is thought to possibly contribute more than half of the $\sim 8\times10^7$ tonnes of volcanic CO_2 released to the atmosphere annually (Brantley and Koepenick, 1995). During periods when no such single volcano predominates, dissolved discharges may be a larger factor in the global output of magmatic carbon.

Conceivably, more magmatic carbon may be transported in low-temperature groundwater than in the much more impressive hydrothermal systems. The hot springs and wells in the Long Valley caldera (Fig. 1) are the subject of numerous studies, many focusing on magmatic degassing (e.g. Hilton, 1996). The caldera geothermal system is large, with a total discharge of 370 l/s according to Sorey et al. (1991), and the fluid is rich in DIC ($\sim$20 mmol/l, Farrar et al., 1985); but these values give a total DIC discharge of 10 000 t/yr, half the amount presently discharged by the cold groundwaters on Mammoth Mountain.

Compared to the widespread occurrence of high-TDS soda springs, dilute CO_2-rich waters may be rare. Examples have been reported in a few areas where CO_2 emissions are high; e.g. Cameroon (Tanyileke et al., 1996) and Azores (Cruz et al., 1999), and in general, they constitute an important sign of abundant free gas in the upper levels of a volcanic edifice accessible to shallow groundwater. However, this type of feature is likely to be overlooked in volcanic studies because the main indication of anomalous [CO_2] is a low pH just at the spring vent. The CO_2 can be rapidly lost in the outflow channel so that the [DIC] downstream, in the form of HCO_3^-, is not particularly large. A careful search for such features should be part of a much needed global investigation of magmatic carbon in cold groundwaters.

7. Conclusions

The cold groundwater system at Mammoth Mountain currently discharges 2×10^4 t/yr of magmatic DIC; that at Lassen discharges at least 1×10^4 t/yr. These large DIC discharges demonstrate the ability of cold groundwater to absorb and transport magmatic CO_2, a so-called 'sparingly soluble gas', at dormant volcanoes. This may be the main reason that incidents of diffuse soil discharge are rarely reported. Only after the groundwater in zones of gas up-flow has been saturated would diffuse emissions begin. The 1×10^5 t/yr of CO_2 that issues from the tree-kill areas at Mammoth Mountain can be viewed as the gas that exceeded the dissolving capacity of the groundwater.

Regardless of how magmatic DIC fits into the global rates of carbon dioxide emission, groundwater transport of magmatic carbon can certainly be an important factor at individual volcanoes. Quantification of DIC discharge can help constrain both weathering and intrusion rates, as was done in this report for Mammoth Mountain. Detailed chemical and isotopic studies not only help quantify the discharge, but also may provide additional insight to subsurface conditions. For example, CO_2-rich groundwaters that are cold and dilute may be a general indicator that a volcano contains a pressurized gas cap. Gas or vapor caps, which can overlie active or fossil hydrothermal reservoirs, must be considered in evaluating the possible hazards during periods of volcanic unrest.

Acknowledgements

We acknowledge Bob Michel and John Radyk for tritium analyses and the employees of the Mammoth Mountain Ski Area and the Mammoth County Water District for access to their wells. Helpful reviews were provided by Lee Davisson, Terry Gerlach, Giovanni Chiodini, and Yousif Kharaka. This work was partly supported by the Director, Office of Energy Research, Office of Basic Energy Sciences, Engineering and Geoscience Division of the U.S. Department of Energy under contract DE-AC03-76SF00098.

References

Allard, P., Carbonelle, J., Dajlevic, D., Le Bronec, J., Morel, P., Robe, M.C., Maurenas, J.M., Faivre-Pierret, R., Martin, D., Sabroux, J.C., Zettwoog, P., 1991. Eruptive and diffuse emissions of CO_2 from Mount Etna. Nature 351, 387–391.

Bailey, R.A., 1989. Geologic Map of the Long Valley Caldera, Mono-Inyo Craters Volcanic Chain, Eastern California. U.S. Geol. Surv. Map I-1933, 11 pp.

Barnes, I., Kistler, R.W., Mariner, R.H., Presser, T.S., 1981. Geochemical Evidence on the Nature of the Basement Rocks of the Sierra Nevada, California. U.S. Geol. Surv. Water-Supply Pap. 2181, 13 pp.

Barnes, I., Irwin, W.P., White, D.E., 1984. Global Distribution of Carbon Dioxide Discharges and Major Zones of Seismicity. U.S. Geol. Surv. Misc. Invest. Map I-1528, 10 pp.

Baubron, J.C., Allard, P., Toutain, J.P., 1990. Diffuse volcanic emissions of carbon dioxide from Vulcano Island, Italy. Nature 344, 51–53.

Baxter, P.J., Baubron, J.-C., Coutinho, R., 1999. Health hazards and disaster potential of ground gas emissions at Furnas volcano. São Miguel, Azores. J. Volcanol. Geotherm. Res. 92, 95–106.

Brantley, S.L., Koepenick, K.W., 1995. Measured carbon dioxide emissions from Oldoinyo Lengai and the skewed distribution of passive volcanic fluxes. Geology 23, 933–936.

Buchanan, T.J., Somers, W.P., 1969. Discharge Measurements at Gaging Stations. U.S. Geol. Surv. Tech. Water Resour. Invest. Bk. 3, ch. A8, 65 pp.

Cerling, T.E., Solomon, D.K., Quade, J., Bowman, J.R., 1991. On the isotopic composition of carbon in soil carbon dioxide. Geochim. Cosmochim. Acta 55, 3403–3405.

Chiodini, G., Frondini, F., Kerrick, D.M., Rogie, J., Parello, F., Peruzzi, L., Zanzari, A.R., 1999. Quantification of deep CO_2 fluxes from Central Italy. Examples of carbon balance for regional aquifers and of soil diffuse degassing. Chem. Geol. 159, 205–222.

Chiodini, G., Frondini, F., Cardellini, C., Parello, F., Peruzzi, L., 2000. Rate of diffuse carbon dioxide Earth degassing estimated from carbon balance of regional aquifers: the case of central Apennine, Italy. J. Geophys. Res. B105, 8423–8434.

Cook, A.C., Hainsworth, L.J., Sorey, M.L., Evans, W.C., Southon, J.R., 2001. Radiocarbon studies of plant leaves and tree rings from Mammoth Mountain, CA: A long-term record of magmatic CO_2 release. Chem. Geol. 177, 117–131.

Cruz, J.V., Coutinho, R.M., Carvalho, M.R., Oskarsson, N., Gislason, S.R., 1999. Chemistry of waters from Furnas volcano, São Miguel, Azores: fluxes of volcanic carbon dioxide and leached material. J. Volcanol. Geotherm. Res. 92, 151–167.

Evans, W.C., Banks, N.G., White, L.D., 1981. Analyses of gas samples from the summit crater. In: Lipman, P.W., Mullineaux, D.R., (Eds.), The 1980 Eruptions of Mount St. Helens, Washington. U.S. Geol. Surv. Prof. Pap. 1250, pp. 227–232.

Evans, W.C., White, L.D., Rapp, J.B., 1988. Geochemistry of some gases in hydrothermal fluids from the southern Juan de Fuca Ridge. J. Geophys. Res. B93, 15305–15313.

Evans, W.C., Sorey, M.L., Michel, R.L., Kennedy, B.M., Hainsworth, L.J., 1998. Gas–water interaction at Mammoth Mountain, California, USA. In: Arehart, G.B., Hulston, J.R. (Eds.), Proc. 9th International Symposium on Water–Rock Interaction. A.A. Balkema, Rotterdam, pp. 443–446.

Evans, W.C., Sorey, M.L., Michel, R.L., Cook, A.C., Kennedy, B.M., Busenberg, E., 2001. Tracing magmatic carbon in groundwater at Big Springs, Long Valley caldera, USA. In: Cidu, R., Fanfani, L. (Eds.), Proc. 10th International Symposium on Water–Rock Interaction. A.A. Balkema, Rotterdam, pp. 803–806.

Farrar, C.D., Sorey, M.L., Rojstaczer, S.A., Janik, C.J., Mariner, R.H., Winnett, T.L., 1985. Hydrologic and Geochemical Monitoring in Long Valley Caldera, Mono County, California, 1982–1984. U.S. Geol. Surv. Water Resour. Invest. Rep. 85–4183, 137 pp.

Farrar, C.D., Sorey, M.L., Rojstaczer, S.A., Janik, C.J., Winnett, T.L., 1987. Hydrologic and Geochemical Monitoring in Long Valley Caldera, Mono County, California, 1985. U.S. Geol. Surv. Water Resour. Invest. Rep. 87-4090, 71 pp.

Farrar, C.D., Sorey, M.L., Evans, W.C., Howle, J.F., Kerr, B.D., Kennedy, B.M., King, C.-Y., Southon, J.R., 1995. Forest-killing diffuse CO_2 emission at Mammoth Mountain as a sign of magmatic unrest. Nature 376, 675–678.

Farrar, C.D., Neil, J.M., Howle, J.F., 1998. Magmatic Carbon Dioxide Emissions at Mammoth Mountain, California. U.S. Geol. Surv. Water Resour. Invest. Rep. 98-4217, 34 pp.

Feth, J.H., Roberson, C.E., Polzer, W.L., 1964. Sources of Mineral Constituents in Water from Granitic Rocks, Sierra Nevada, California and Nevada. U.S. Geol. Surv. Water-Supply Pap. 1535-I, 70 pp.

Friedman, I., O'Neil, J.R., 1977. Compilation of Stable Isotope Fractionation Factors of Geochemical Interest. U.S. Geol. Surv. Prof. Pap. 440-KK, 12 pp.

Gerlach, T.M., Doukas, M.P., McGee, K.A., Kessler, R., 2001. Soil efflux and total emission rates of magmatic CO_2

at the Horseshoe Lake tree kill, Mammoth Mountain, California, 1995–1999. Chem. Geol. 177, 101–116.

Gerlach, T.M., Doukas, M.P., McGee, K.A., Litasi-Gerlach, A., Sutton, J.A., Elias, T., 1996. Ground efflux of 'cold' CO_2 in the Long Valley caldera and Mono-Inyo Craters volcanic chain of eastern California. EOS Trans. AGU 77, F830.

Gerlach, T.M., Doukas, M.P., McGee, K.A., Kessler, R., 1999. Airborne detection of diffuse carbon dioxide emissions at Mammoth Mountain, California. Geophys. Res. Lett. 26, 3661–3664.

Giammanco, S., Gurrieri, S., Valenza, M., 1998. Anomalous soil CO_2 degassing in relation to faults and eruptive fissures on Mount Etna (Sicily, Italy). Bull. Volcanol. 60, 252–259.

Giggenbach, W.F., 1988. Geothermal solute equilibria. Derivation of Na–K–Mg–Ca geoindicators. Geochim. Cosmochim. Acta 52, 2749–2765.

Gleason, J.D., Friedman, I., Hanshaw, B.B., 1969. Extraction of Dissolved Carbonate Species from Natural Water for Carbon-Isotope Analysis. U.S. Geol. Surv. Prof. Pap. 650-D, pp. 248–250.

Heim, K., 1991. Hydrologic Study of the Big Springs, Mono County, California, senior thesis prepared for Mammoth County Water District, Mammoth Lakes, California. Calif. State Univ., Fullerton, 79 pp.

Hem, J.D., 1985. Study and Interpretation of the Chemical Characteristics of Natural Water. U.S. Geol. Surv. Water-Supply Pap. 2254, 263 pp.

Hilton, D.R., 1996. The helium and carbon isotope systematics of a continental geothermal system: results from monitoring studies at Long Valley caldera (California, USA). Chem. Geol. 127, 269–295.

Hiyagon, H., Kennedy, B.M., 1992. Noble gases in CH_4-rich gas fields, Alberta, Canada. Geochim. Cosmochim. Acta 56, 1569–1589.

James, E.R., Manga, M., Rose, T.P., 1999. CO_2 degassing in the Oregon Cascades. Geology 27, 823–826.

Kennedy, B.M., Lynch, M.A., Reynolds, J.H., Smith, S.P., 1985. Intensive sampling of noble gases in fluids at Yellowstone, I. Early overview of the data, regional patterns. Geochim. Cosmochim. Acta 49, 1251–1261.

Kharaka, Y.K., Gunter, W.D., Aggarwal, P.K., Perkins, E.H., DeBraal, J.D., 1988. SOLMINEQ.88: A Computer Program for Geochemical Modeling of Water–Rock Interactions. US Geol. Surv. Water Resour. Invest. Rep. 88-4227, 420 pp.

Kroopnick, P., 1974. The dissolved O_2–CO_2–^{13}C system in the eastern equatorial Pacific. Deep Sea Res. 21, 211–227.

McGee, K.A., Gerlach, T.M., 1998. Annual cycle of magmatic CO_2 in a tree kill at Mammoth Mountain: implications for soil acidification. Geology 26, 463–466.

Pearson, F.J., Fisher, D.W., Plummer, L.N., 1978. Correction of ground-water chemistry and carbon isotopic composition for effects of CO_2 outgassing. Geochim. Cosmochim. Acta 42, 1799–1807.

Presser, T.S., Barnes, I., 1974. Special Techniques for Determining Chemical Properties of Geothermal Waters. U.S. Geol. Surv. Water Resour. Invest. Rep. 22-74, 11 pp.

Rahn, T.A., Fessenden, J.E., Wahlen, M., 1996. Flux chamber measurements of anomalous CO_2 emission from the flanks of Mammoth Mountain, California. Geophys. Res. Lett. 23, 1861–1864.

Reid, J.B., Jr., Reynolds, J.L., Connolly, N.T., Getz, S.L., Polissar, P.J., Winship, L.J., 1998. Carbon isotopes in aquatic plants, Long Valley caldera, California as records of past hydrothermal and magmatic activity. Geophys. Res. Lett. 25, 2853–2856.

Rose, T.P., Davisson, M.L., 1996. Radiocarbon in hydrologic systems containing dissolved magmatic carbon dioxide. Science 273, 1367–1370.

Rose, T.P., Davisson, M.L., Criss, R.E., 1996. Isotope hydrology of voluminous cold springs in fractured rock from an active volcanic region, northeastern California. J. Hydrol. 179, 207–236.

Shevenell, L., Goff, F., Grigsby, C.O., Janik, C.J., Trujillo, P.E., Jr., Counce, D., 1987. Chemical and isotopic characteristics of thermal fluids in the Long Valley caldera lateral flow system, California. Trans. Geotherm. Resour. Council 11, 195–201.

Sorey, M.L., Suemnicht, G.A., Sturchio, N.C., Nordquist, G.A., 1991. New evidence on the hydrothermal system in Long Valley caldera, California, from wells, fluid sampling, electrical geophysics, and age determinations of hot-spring deposits. J. Volcanol. Geotherm. Res. 48, 229–263.

Sorey, M.L., Kennedy, B.M., Evans, W.C., Farrar, C.D., Suemnicht, G.A., 1993. Helium isotope and gas discharge variations associated with crustal unrest in Long Valley caldera, California. J. Geophys. Res. B98, 15871–15889.

Sorey, M.L., Evans, W.C., Kennedy, B.M., Farrar, C.D., Hainsworth, L.J., Hausback, B., 1998. Carbon dioxide and helium emissions from a reservoir of magmatic gas beneath Mammoth Mountain, California. J. Geophys. Res. 103, 15303–15323.

Sorey, M., Evans, B., Kennedy, M., Rogie, J., Cook, A., 1999. Magmatic gas emissions from Mammoth Mountain. Calif. Geol. 52, 4–16.

Tanyileke, G.Z., Kusakabe, M., Evans, W.C., 1996. Chemical and isotopic characteristics of fluids along the Cameroon Volcanic Line, Cameroon. J. Afr. Earth Sci. 22, 433–441.

Werner, C., Brantley, S.L., Boomer, K., 2000. CO_2 emissions related to the Yellowstone volcanic system 2. Statistical sampling, total degassing, and transport mechanisms. J. Geophys. Res. B105, 10831–10846.

White, A.F., Petersen, M.L., Wollenberg, H., Flexser, S., 1990. Sources and fractionation processes influencing the isotopic distribution of H, O, and C, in the Long Valley hydrothermal system, California, USA. Appl. Geochem. 5, 571–585.

Williams-Jones, G., Styx, J., Heiligmann, M., Charland, A., Sherwood Lollar, B., Arner, N., Garzon, G., Barquero, J., Fernandez, E., 2000. A model of diffuse degassing at three subduction-related volcanoes. Bull. Volcanol. 62, 130–142.